Analytica Chimica Acta 817 (2014) 42–47

Contents lists available at ScienceDirect

Analytica Chimica Acta

journal homepage: www.elsevier.com/locate/aca

Label-free fluorescent biosensor based on the target recycling and Thioflavin T-induced quadruplex formation for short DNA species of c-erbB-2 detection

Jinghua Chen[a], Jia Lin[a], Xi Zhang[a], Shuxian Cai[a], Dongzhi Wu[a], Chunyan Li[a], Sheng Yang[b,*], Jing Zhang[c,*]

[a] Department of Pharmaceutical Analysis, Faculty of Pharmacy, Fujian Medical University, Fuzhou, Fujian 350004, China
[b] Department of Medical Oncology, Fujian Medical University Union Hospital, Fujian Key Laboratory of Tumor Translational Medicine, Fuzhou 350001, China
[c] Department of Chemistry and Biology, Faculty of Life Science, Fujian Agriculture and Forestry University, Fuzhou, Fujian 350002, China

HIGHLIGHTS

- The biosensor was based on target recycling and Thioflavin T-induced quadruplex.
- Thioflavin T was first used as a fluorescent indicator for biosensor fabrication.
- This sensor can detect as low as 20 fM DNA with ultra-high discrimination ability.

GRAPHICAL ABSTRACT

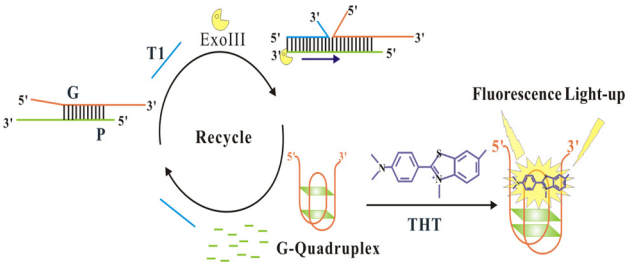

ARTICLE INFO

Article history:
Received 22 October 2013
Received in revised form 20 January 2014
Accepted 26 January 2014
Available online 10 February 2014

Keywords:
Fluorescent biosensor
Target recycling
Thioflavin T
Quadruplex
c-erbB-2
Saliva

ABSTRACT

Non-invasive early diagnosis of breast cancer is the most effective way to improve the survival rate and increase more chances of breast-conserving. In this paper, we developed a label-free fluorescent biosensor based on nuclease assisted target recycling and Thioflavin T-induced quadruplex formation for short DNA species of c-erbB-2 detection in saliva. By employing the strategy, the sensor can detect as low as 20 fM target DNA with high discrimination ability even against single-base mismatch sequence. To the best of our knowledge, the proposed sensor is the first attempt to apply Thioflavin T that possesses outstanding structural selectivity for G-quadruplex in DNA amplification techniques, which may represent a promising path toward direct breast cancer detection in saliva at the point of care.

© 2014 Elsevier B.V. All rights reserved.

1. Introduction

Breast cancer, comprising 22.9% of all cancer types, is the most common cancer among women worldwide with the morbidity rising year by year [1]. Early diagnosis is the most effective way to improve survival rate, reduce the suffering and the cost, and increase more chances of breast-conserving for the patients with breast cancer [2]. Compared with the commonly used clinical

* Corresponding authors. Tel.: +86 591 83769155; fax: +86 591 83769155.
E-mail addresses: yangshjxh@126.com (S. Yang), 1601225385@qq.com (J. Zhang).

0003-2670/$ – see front matter © 2014 Elsevier B.V. All rights reserved.
http://dx.doi.org/10.1016/j.aca.2014.01.053

diagnosis of breast cancer, such as mammography, ultrasonography, magnetic resonance imaging (MRI), and positron emission tomography (PET) [3], the accurate detection of tumor markers in biosamples has been considered as an ideal method in early stage due to higher sensitivity, non-invasiveness, low price, simplicity and speed. With the recent development of proteomic technologies, various tumor markers have been identified and employed for breast cancer detection [4]. Present studies suggest that soluble fragments of the c-erbB-2 oncogene, located on chromosome 17, q21, can be released from the cell surface and become detectable in patients with breast cancer [5]. Especially, the c-erbB-2 oncogene was reported to be equal to or surpass the ability of CA 15-3 ("gold standard" of breast cancer diagnosis) for early diagnosis and/or follow-up recurrent screening of breast cancer [5]. It is worth noting that Streckfus et al. found the c-erbB-2 presented not only in serum but also in saliva of the breast cancer patients [6]. Compared with the serum, the whole saliva is simpler to collect and store as well as obtained more easily in sufficient quantities for testing. Furthermore, the non-invasive collection method of saliva reduces anxiety and discomfort, thereby ameliorating testing antipathy and promoting more frequent screening events [7]. In addition, the levels of interfering materials (cells, DNA, RNA and proteins) and inhibitory substances are lower and less complex in saliva than in serum. More importantly, single nucleotide polymorphism (SNP) detection from saliva DNA has been proposed to offer higher accuracy than blood based analysis [8]. Despite the obvious advantages, a number of notable challenges associated with diagnostic technique in saliva still exist, such as low levels of salivary tumor markers and high levels of mucins and proteolytic enzymes. However, the commonly used diagnostic tests for c-erbB-2 oncogene, including southern blot, slot blot, dot blot analyses, polymerase chain reaction, in situ hybridization and fluorescent in situ hybridization (FISH) [9–12], are low sensitive, complicated, time-consuming, high cost as well as high risk of false positive and false negative. Therefore, there is still a compelling need for sensitive and specific, simple, rapid methods for c-erbB-2 oncogene detection.

Fluorescent biosensor has been recognized as a promising tool for clinical diagnostics due to its many appealing advantages, including high sensitivity, low cost, easy-to-perform, remote control and biocompatibility [13]. However, due to the low concentration of c-erbB-2 oncogene and the complex background of saliva, conventional fluorescent biosensors do not meet the clinical diagnostic requirement for direct c-erbB-2 oncogene detection in saliva. To increase analytical sensitivity, many DNA amplification techniques have been reported. Specifically, Li et al. developed a signal amplification scheme based on target-dependent cleavage by a DNA nicking enzyme, bringing the detection limit down to tens of femtomolar [14]. Nevertheless, the nicking enzyme signal amplifications require target DNA with a specific sequence for enzyme recognition, which hampers the further use for general applications. In contrast, Zuo et al. developed a versatile signal amplification scheme based on a sequence-independent enzyme (Exo III)-aided target recycling [15]. Unfortunately, the prerequisite complex and expensive dye-modified procedure limit its practical use. To overcome the shortcomings of the above method, Zhao et al. developed a label-free and general amplified DNA detection system based on Exo III assisted strand-cleavage cycle and ligand-responsive quadruplex formation [16]. Although the label-free sensor was simple in design and fast in operation, the detection limit of the strategy had remained in need of further improvement for practical applications. Furthermore, the optimum power of hydrogen condition of the sensor made it not appropriate for biomedical utilization.

Surprisingly, Mohanty et al. demonstrated for the first time that water soluble Thioflavin T (ThT) was a G-quadruplex specific fluorescent indicator among other DNA forms including single-strand, duplexes or triplexes. It is weakly fluorescent by itself, but exhibits great fluorescence enhancement upon inducing DNA folding into quadruplex under physiological salt conditions. The extraordinary structural selectivity for G-quadruplexes makes ThT as a potential candidate for diagnostic and therapeutic applications [17].

Spurred on by all above findings, herein a label-free fluorescent biosensor based on the Exo III assisted target recycling and ThT-induced quadruplex formation was developed for amplified detection of short DNA species of c-erbB-2 oncogene (T1). Using this biosensor, it was possible to detect T1 through a linear dynamic range of 100 fM to 1 pM with a detection limit down to 20 fM. As far as we know, this is the first attempt to design a signal amplification scheme using ThT as signal transducers for DNA determination, which may represent a promising path toward sensitive, simple, fast and economic early diagnosis of breast cancer.

2. Experimental

2.1. Reagents and apparatus

Oligonucleotides designed in this study were synthesized by Shanghai Sangon Biotechnology Co., which were all purified by HPLC and confirmed by mass spectrometry. The concentrations were quantified by OD260 based on their individual absorption coefficients. Each oligonucleotide was heated to 90 °C for 5 min and slowly cooled down to room temperature before use. Their base sequences were illustrated in Table S1. ThT (3,6-dimethyl-2-(4-dimethylaminophenyl) benzo-thiazolium cation), obtained from Sigma–Aldrich, was purified by column chromatography using a silica gel column and mildly acidic methanol as the eluent. Exonuclease III was purchased from Thermo scientific and used without further purification. Other chemicals were purchased from Sigma-Aldrich and used without further purification. All water used to prepare buffer solutions was obtained by using a Milli-Q water system. All measurements were performed in reaction buffer (50 mM Tris–HCl, 50 mM KCl, 10 mM $MgCl_2$, pH 7.2) unless stated otherwise.

The real saliva sample of breast cancer patient (confirmed by pathological examinations) was obtained from Fujian Medical University Union Hospital (Fujian, China). Signed informed consent was obtained from the patient participating in the study before surgery.

Fluorescence spectra (Varian Cary Eclipse Fluorimeter, Varian, Inc. Agilent Technologies) were measured with a Peltier block, using quartz fluorescence cuvettes (4 mm × 10 mm; Sub-micro, 50 μL), and with the following settings: λ_{ex} = 425 nm, λ_{em} = 485 nm, 5 nm slit, PMT detector voltage = 600 V. UV–vis absorbance spectra were measured with a UV-2501PC spectrophotometer (SHIMADZU, Japan) using a quartz cell with 1.0 cm optical pathway. The circular dichroism (CD) spectra were studied based on the Jasco J-810 CD spectropolarimeter (Tokyo, Japan). The optical chamber (1 cm path length, 500 μL volume) was deoxygenated with dry purified nitrogen (99.99%) before use and kept in the nitrogen atmosphere during experiments. Three scans (100 nm min^{-1}) from 220 nm to 330 nm at 0.1 nm intervals were accumulated and averaged. The background of the buffer solution was subtracted from the CD data.

2.2. Preparation of the fluorescent biosensor for T1 detection

Different concentrations of T1 were mixed and reacted with 50 μL of reaction buffer containing 10 μM G/P probe, 5 μM THT and 50 U Exo III at 37 °C for 40 min, respectively. The fluorescence spectra of the above resulted solutions were recorded in the wavelength range from 435 nm to 600 nm with the excitation of 425 nm at room temperature.

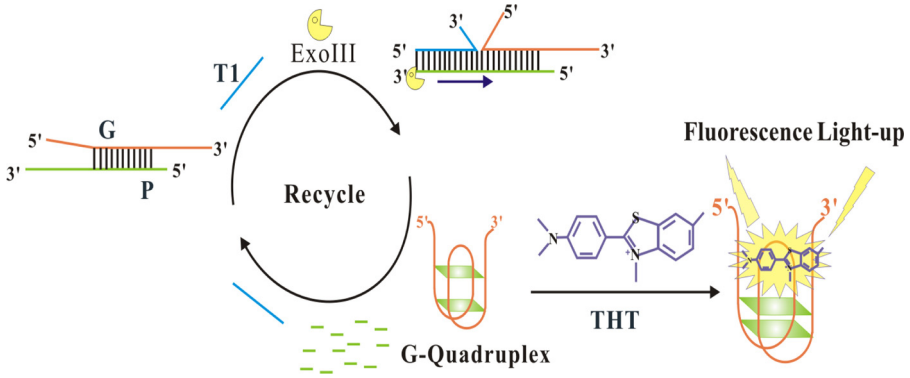

Fig. 1. Schematic illustration of the sensor for amplified DNA detection.

2.3. The preparation of artificial saliva sample

Un-stimulated saliva samples were collected between 9 a.m. and 10 a.m. with previously established protocols [18]. Subjects were asked to refrain from eating, drinking, smoking, or oral hygiene procedures for at least 1 h before the collection. Saliva samples were centrifuged at 603 × *g* for 10 min at 4 °C. Then, the 1 mL of supernatant liquid was taken and diluted to 100 mL with buffer solution. The different concentrations of T1 were then added into the diluted saliva to prepare artificial saliva samples and the concentrations of T1 in the samples were determined with our biosensor.

3. Results and discussion

3.1. Experimental principle of the biosensor

Herein, we develop a label-free and ultra-highly sensitive and selective biosensor for amplified short DNA species of c-erbB-2 oncogene detection by combining Exo III assisted target recycling with ThT-induced quadruplex formation. As shown in Fig. 1, the DNA detection system contains ThT, Exo III and a linear double stranded DNA (dsDNA) probe. As mentioned above, ThT is a water-soluble fluorogenic dye characterized by a pronounced structural selectivity for G-quadruplexes but not for single, double or triplexes stranded DNA. Exo III has a double strand-specific which selectively digesting dsDNA from 3′-OH blunt or recessed end. The linear dsDNA probe consists of two partially complementary oligonucleotides (P and guanines-rich G) with protruding 3′-terminus to hinder the digestion of Exo III. Initially, the fluorescent signal is low owing to the weak interaction between the dsDNA probe and ThT. Upon addition of T1, the hybridization between dsDNA probe and T1 leads to a blunt 3′-terminus in dsDNA probe. Therefore, Exo III can stepwise digest the dsDNA probe from this blunt terminus while releasing T1 and G. Then in the presence of ThT and monovalent ions, the released G folds into a quadruplex structure accompanied by a pronounced enhancement of fluorescence intensity due to the strong interaction between the quadruplex and ThT. At the same time, the released T1 can hybridize with another dsDNA probe, whence the cycle starts anew. Thus, a single copy of T1 ultimately induces many G folding into quadruplex to bind with ThT, leading to significant amplification of the fluorescent signal. Using this sensing platform, an ultra-highly sensitive and selective, simple, rapid sensor for the amplified DNA detection has been developed.

3.2. Identification of quadruplex formation by CD

CD spectroscopy is a very useful tool for the detection and characterization of G-quadruplexes. Signature CD spectra have been reported for many DNA structures including dsDNA and G-quadruplex species [19]. We used CD to investigate the feasibility of our strategy at first. As shown in Fig. 2, the CD spectrum of G/P gives a clear CD signal with a positive peak at 265 corresponding to base stacking, and one negative peak at around 240 nm corresponding to helicity, indicating a definite two-helical structure (G/P dsDNA probe, curve b) [20]. The addition of ThT does not change the CD spectrum obviously due to the weak interaction between ThT and duplexes DNA (curve c). Upon T1 addition, the hybridization of G/P dsDNA probe with T1 leads to a more stable two-helical structure of G/P/T1 with the intensity of positive peak at 265 nm increased (curve a). When G/P/T1 is degraded by Exo III, a dramatic change is observed with a positive peak at 295 nm appeared (the typical characteristics CD spectra of antiparallel G-quadruplex [21] and the band near 265 nm obviously decrease in the meantime) (curve d). These results indicate the two-helical structure was digested and the G-quadruplex definitely formed in the presence of ThT and monovalent ions. As a control experiment, CD spectrum of G and ThT solution was tested. As shown in curve e, in the presence of ThT, G folds exclusively into an antiparallel quadruplex with a characteristic CD peak at 295 nm and a trough at 265 nm (curve e). All above CD results confirm that our biosensor indeed works as we expect.

3.3. Identification of quadruplex formation by UV–vis and fluorescent spectrum

To further validate our approach, we use the UV–vis spectrum to investigate absorbance changes of our detection system. As Fig. 3A shows, in dilute solution of ThT (5 μM) reaction buffered at pH 7.2, the ThT dye displays its characteristic absorption profile with a maximum at 412 nm (curve a). The addition of P or G/P leads to

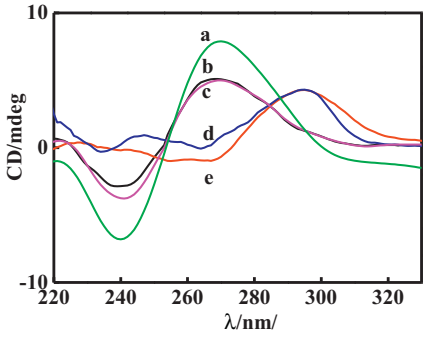

Fig. 2. CD spectra of G/P/T + ThT (a), G/P (b), G/P + ThT (c), G/P/T + ThT + Exo III (d), G + ThT (e) in reaction buffer. The concentrations of G, P, T1, ThT and Exo III were 10 μM, 10 μM, 1 pM, 5 μM, and 50 U, respectively.

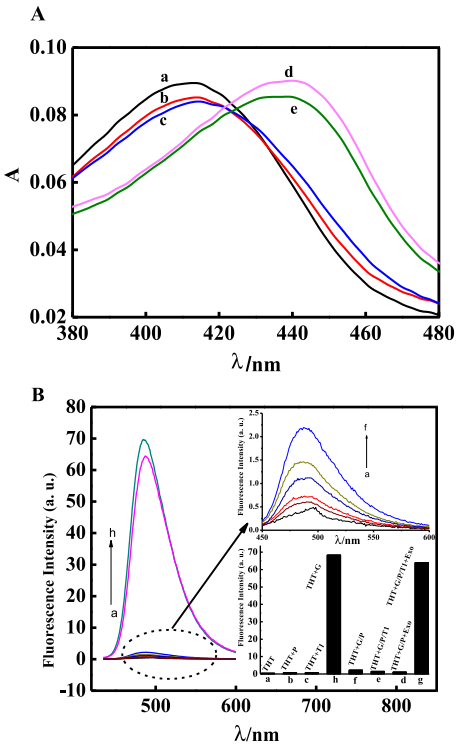

Fig. 3. (A) UV–vis spectra of ThT (a) in the presence of P (b), G/P (c), G/P/T1 + Exo III (d) and G (e) in reaction buffer, respectively. The experimental conditions were same as that in Fig. 2. (B) Fluorescence spectra of ThT (a) in the presence of P (b), T1 (c), G/P + Exo III (d), G/P/T1 (e), G/P (f), G/P/T1 + Exo III (g) and G (h) in reaction buffer, respectively. The experimental conditions were same as that in Fig. 2.

hypochromism and bathochromic shift under the same conditions (curve b and curve c). These results indicate that the interaction between ThT and single-strand or duplexes DNA is electrostatic interaction between the positively charged groups of the ThT and the negatively charged phosphate groups of the DNA. Therefore, ThT may still remain flexible orientations and may not show greatly absorbance changes [17]. When the G/P/T1 is degraded by Exo III, obvious red shift (the absorption peak at 412 nm shifted to 441 nm) is observed (curve d), indicating corresponding changes of DNA conformation and structure. As discussed above, the hybridization of T1 leads a blunt 3′-terminus in G/P duplexes. Then Exo III can catalyze the stepwise removal of mononucleotides from the G/P/T1 system, ultimately releasing T1 and G. In the presence of ThT and monovalent ions, the released G folds into quadruplex structure. Due to the binding sites of ThT in the quadruplexes are more specific and rigid, an obvious red shift in the UV–vis spectrum is observed here [17]. As a contrast experiment, UV–vis spectrum of G and ThT solution was tested. As shown in curve e, the absorption band of ThT solution bathochromically shifts to 442 nm (Fig. 3A, curve e), pointing out a strong interaction between ThT and G strand. The phenomenon might account for the foundation of the mechanism suggested by Mohanty et al., who reported that ThT could induce G-rich DNA strand fold into quadruplex structure in the presence tris buffer [17]. All above UV–vis results also confirm that our biosensor indeed works as we expect.

The fluorescence measurements are also performed to serve as a proof of concept to test the principle of our design. As Fig. 3B shows, the ThT displays a very weak fluorescent emission profile centered at 492 nm (curve a). Moreover, the fluorescent intensities of the samples containing no T1 and Exo III are nearly close to that of ThT, indicating that no ThT responsive quadruplex formed (curve b, c, d, e, f). It is worth noting that the fluorescence intensity does not enhance even in the presence of T1 or Exo III, respectively. However,

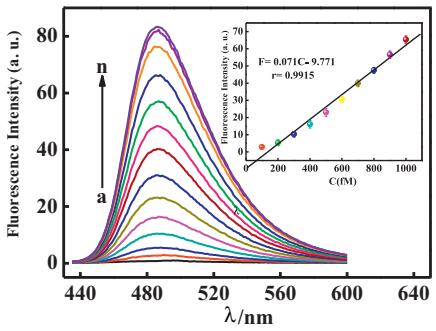

Fig. 4. Fluorescence emission spectra of ThT + G/P in the presence of Exo III and various concentrations of T1 (from a to n): 0.00 fM, 100 fM, 200 fM, 300 fM, 400 fM, 500 fM, 600 fM, 700 fM, 800 fM, 900 fM, 1 pM, 5 pM, 10 pM, 50 pM. Inset: A calibration curve demonstrating peak fluorescence intensity versus T1 concentration.

upon T1 and Exo III addition simultaneously, a great fluorescence enhancement can be achieved (curve g). These results indicate that the T1 can be acted as a trigger of the Exo III digestion reaction and liberate G to fold into quadruplex. Due to the binding sites in the quadruplexes are more specific and rigid for ThT, the fluorescence intensity increases dramatically. As a contrast experiment, the sample containing only G and ThT was tested. As shown in curve h, its fluorescence intensity is almost close to curve g, demonstrating the formation of ThT responsive quadruplex in our detection system. All above fluorescence measurements confirm the feasibility of the presented biosensor.

3.4. The sensitivity of the biosensor

The sensitivity of the proposed fluorescent biosensor for accurate quantification of T1 is investigated by varying the concentration of T1 under the optimized assay conditions. As shown in Fig. 4, a dramatic increase of fluorescence intensity is observed as the concentration of T1 increase from 100 fM to 50 pM. Meanwhile, the intensity is linear to the concentration of T1 in the range from 100 fM to 1 pM (Fig. 4, inset) with a detection limit (taken to be three times the standard deviation of 10 blank measurements) of 20 fM. The repeatability of the biosensor was assessed by analyzing 500 fM target DNA and the relative standard deviation (RSD) of eight replicate determinations was 1.46%.

Compared with the work reported by Qu et al. [16], our sensor has higher sensitivity due to the following factors. On the one hand, the G-rich DNA probe we designed has more mismatched bases at 5′-terminus, which make the strand replacement reaction easier. Therefore, the fewer target DNA is able to trigger the whole cycle reaction successfully, resulting in an increment in sensitivity. On the other hand, in comparison with NMM used in Qu et al. assay, the ThT we used possess higher structural selectivity for G-quadruplexes, which leads to lower background signal and higher sensitivity. Furthermore, compared with some existing signal amplification methods requiring chemical modification [15,22,23], the proposed biosensor not only contains no label and purification processes but also is more sensitive, easy-to-perform, inexpensive and fast. Furthermore, the sensitivity of the biosensor is also more than three orders of magnitude higher than that of reported label-free enzymatic amplification sensors due to the extraordinary selectivity for quadruplex of ThT [16].

3.5. The selectivity of the method

The selectivity of this amplified sensor is investigated with various DNA sequences (perfectly complementary target T1, single-base-mismatched T2, double-base-mismatched T3, Three-base

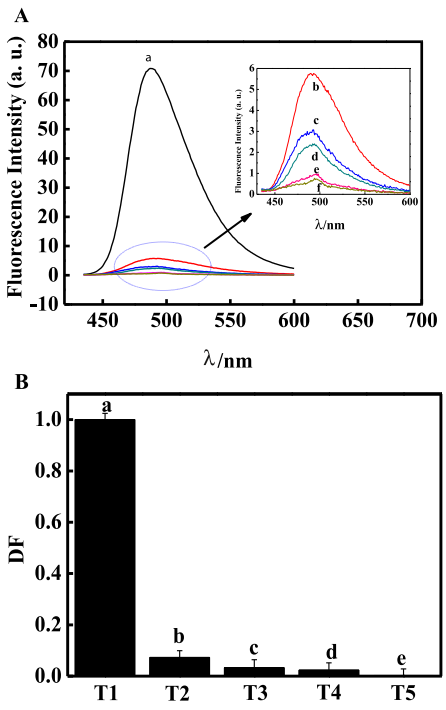

Fig. 5. (A) Specificity of the DNA assay detecting different target: (a) T1, (b) T2, (c) T3, (d) T4, (e) T5, (f) no target DNA was added. (B) The DF obtained with different sequences: (a) T1, (b) T2, (c) T3, (d) T4, (e) T5. The concentrations of T2, T3, T4 and T5 were all 1 pM. Other experimental conditions were same as that in Fig. 2.

mismatched T4 and non-complementary T5). As shown in Fig. 5A, an obvious fluorescence enhancement is obtained in the addition of T1. However, the enhanced intensities for T2, T3 or T4 are sharply decreased. Non-complementary T5 DNA shows nearly no response. In order to demonstrate the discrimination ability of the amplified sensor, we define the discrimination factor (DF) as $(F_2 - F_0)/(F_1 - F_0)$, where F_1, F_2 and F_0 are the fluorescence intensities produced by the addition of complementary target (T1), mismatched target (T2–T5) and the background (without target), respectively. The smaller DF indicates the higher specificity. As shown in Fig. 5B, DF for mismatched DNA decreases obviously as compared with that for the complementary target. This result clearly indicates that the proposed detection platform has excellent discrimination ability even against single-base mismatch. This high specificity is probably because the weak hybridization of mismatched DNA with duplex probe and the weak Exo III digestion for the mismatched DNA hybrid duplex probe. To sum up, compared with previous fluorescent and electrochemical biosensors based on signal amplification scheme, our sensor has better discrimination ability even against single-base mismatch and higher sensitivity due to the high selectivity of ThT for G-quadruplex (see Table S2).

3.6. Optimization of experimental conditions

Experimental variables affecting the whole sensing process are optimized. The temperature of the detection system will directly affect not only the hybridization efficiency of G/P/T1 but also the digestion activity of the Exo III. So, first, the temperature of the detection system is investigated. Figure S1A shows the relationship between the temperature of the system and the fluorescence intensity. From Figure S1A, it is clearly observed that the fluorescence intensity firstly increases and then decreases with the increase of the temperature. Considering the fact that the theoretical hybridization temperature of DNA is about 40 °C and the Exo III has the highest enzymatic activity at the temperature of 30–37 °C, 37 °C is used for subsequent detection.

Second, the ThT concentration is optimized by recording the fluorescence intensity with T1 at different concentration of ThT. As shown in Figure S1B, the optimum ThT concentration is 5 μM according to the best signal-to-noise level.

Third, we incubate the DNA detection system with various concentrations of Exo III (0–100 U). We observe that the fluorescence intensity of ThT increase as the concentration of Exo III increase and reach the maximum at 50 U (Figure S1C). Then the emission intensity of the ThT decreases slowly [24].

In addition, the incubation time is assayed from 0 to 2 h. The fluorescence intensity reaches a stable value at times longer than 40 min, so the value is chosen for further studies (Figure S1D). Finally, the effect of other experimental variables such as buffer type and pH of the buffer are also examined in detail. The results show that the optimum conditions are Tris–HCl and 7.2 (Figure S1E), respectively.

Table 1
Determination of T1 in artificial saliva samples ($n = 5$).

T1 added (fM)	Detected conc. (fM)	Recovery (%)	RSD (%)
200	224	112	1.2
500	540	108	1.6
1000	988	98.8	1.4

3.7. Detection of artificial saliva sample

In order to evaluate the applicability, the saliva samples spiked with different concentrations of T1 are detected with our biosensor. The results shown in Table 1 indicate that our biosensor has a strong resistance to the complex matrix of saliva, and can be used to detect ultra-trace amounts of T1 in real saliva samples.

3.8. Detection of real sample

To determine whether this method could be applied in the detection of real sample, we first prepared a real saliva sample of breast cancer patient (confirmed by pathological examinations). The concentration of target DNA in the real sample was measured by the RT-PCR. Then various concentrations of target DNA were spiked into the real sample and detected effectively by our method, respectively. As shown in Table S3, the method reveals the good recovery rates of standard addition from 93.9 to 114%, which indicated that our sensor provide great potential in the clinic diagnosis.

4. Conclusions

A label-free, simple, ultra-highly sensitive and selective fluorescent biosensor based on nuclease assisted target recycling and ThT-induced quadruplex formation for short DNA species of c-erbB-2 detection was developed here. The sensor can detect as low as 20 fM target DNA and exhibits ultrahigh discrimination ability even for the detection of single-base mismatch. These features, as well as its other advantages, such as label-free, easy-to-use, fast and inexpensive technique, make it a promising candidate for a non-invasive early diagnosis for breast cancer detection in saliva, especially in developing parts of the world where lack adequate medical facilities. It must be mentioned that, with more and more tumor markers are found, we envision that our strategy would offer a universal approach for noninvasive and early diagnosis of many kinds of cancer just by designing rational DNA probe according to the target sequence.

Acknowledgements

The authors gratefully acknowledge the financial support of the National Natural Science Foundation of China (21375017, 21205015, 21105012), the National Science Foundation for Distinguished Young Scholars of Fujian Province (2013J06003), the Key Project of Fujian Science and Technology (2013Y0045), National Science Foundation of Fujian Province (2011J01028), Program for Fujian University Outstanding Youth Scientific Research (JA11105, JA10295), Program for New Century Excellent Talents of Colleges and Universities in Fujian Province (JA13130), the Foundation of Fuzhou Science and Technology Bureau (2012-S-148).

Appendix A. Supplementary data

Supplementary data associated with this article can be found, in the online version, at http://dx.doi.org/10.1016/j.aca.2014.01.053.

References

[1] P. Boyle, B. Levin, International Agency for Research on Cancer, World Cancer Report, 2008.
[2] N. Berois, M. Varangot, B. Aizen, R. Estrugo, L. Zarantonelli, P. FernaÂdez, G. Krygier, F. Simonet, E. Barrios, I. MuseÂ, E. Osinaga, Eur. J. Cancer 36 (2000) 717–723.
[3] S.J. Lord, W. Lei, P. Craft, J.N. Cawson, I. Morris, S. Walleser, A. Griffiths, S. Parker, N. Houssami, Eur. J. Cancer 43 (2007) 1905–1917.
[4] J.A. Ludwig, J.N. Weinstein, Nat. Rev. Cancer 5 (2005) 845–856.
[5] C. Streckfus, L. Bigler, T. Dellinger, X. Dai, A. Kingman, J.T. Thigpen, Clin. Cancer Res. 6 (2000) 2363–2370.
[6] C.F. Streckfus, L. Bigler, M. Tucci, J.T. Thigpen, Cancer Invest. 18 (2000) 101–109.
[7] H.P. Lawrence, J. Can. Dent. Assoc. 68 (2002) 170–174.
[8] B.G. Zimmermann, D.T. Wong, Oral Oncol. 44 (2008) 425–429.
[9] D.J. Slamon, W. Godolphin, L.A. Jones, J.A. Holt, S.G. Wong, D.E. Keith, W.J. Levin, S.G. Stuart, J. Udove, A. Ullrich, Science 244 (1989) 707–712.
[10] O.P. Kallioniemi, A. Kallioniemi, W. Kurisu, A. Thor, L.C. Chen, H.S. Smith, F.M. Waldman, D. Pinkel, J.W. Gray, Proc. Natl. Acad. Sci. USA 89 (1992) 5321–5325.
[11] T.L. Gramlich, C. Cohen, C. Fritsch, P.B. DeRose, T. Gansler, Am. J. Clin. Pathol. 101 (1994) 493–499.
[12] K.L. Smith, P.D. Robbins, H.J. Dawkins, J.M. Papadimitriou, S.L. Redmond, S. Carrello, J.M. Harvey, G.F. Sterrett, Hum. Pathol. 25 (1994) 413–418.
[13] S.Y. Chung, S.W. Nam, J. Lim, S. Park, J. Yoon, Chem. Commun. 20 (2009) 2866–2868.
[14] J.J. Li, Y. Chu, B.Y. Lee, X.S. Xie, Nucleic Acids Res. 36 (2008) e36.
[15] X. Zuo, F. Xia, Y. Xiao, K.W. Plaxco, J. Am. Chem. Soc. 132 (2010) 1816–1818.
[16] C. Zhao, L. Wu, J. Ren, X. Qu, Chem. Commun. 47 (2011) 5461–5463.
[17] J. Mohanty, N. Barooah, V. Dhamodharan, S. Harikrishna, P.I. Pradeepkumar, A.C. Bhasikuttan, J. Am. Chem. Soc. 135 (2013) 367–376.
[18] M. Navazesh, Ann. N. Y. Acad. Sci. 694 (1993) 72–77.
[19] H. Kuang, W. Chen, D.H. Xu, L.G. Xu, Y.Y. Zhu, L.Q. Liu, H.Q. Chu, C.F. Peng, C.L. Xu, S.F. Zhu, Biosens. Bioelectron. 26 (2010) 710–716.
[20] Z. Zhang, W. Huang, J. Tang, E. Wang, S. Dong, Biophys. Chem. 97 (2002) 7–16.
[21] P. Balagurumoorthy, S.K. Brahmachar, J. Biol. Chem. 269 (1994) 21858–21869.
[22] Z.L. Pianowski, N. Winssinger, Chem. Commun. 37 (2007) 3820–3822.
[23] C. Shi, C. Zhao, Q. Guo, C. Ma, Chem. Commun. 47 (2011) 2895–2897.
[24] C.H. Leung, D.S. Chan, B.Y. Man, C.J. Wang, W. Lam, Y.C. Cheng, W.F. Fong, W.L. Hsiao, D.L. Ma, Anal. Chem. 83 (2011) 463–466.